Supporting Information for

Molecular-Level Understanding of Continuous Growth from Iron-Oxo Clusters to Iron Oxide Nanoparticles

Hogeun Chang,[†,‡,§] Byung Hyo Kim,[†,‡,§] Hu Young Jeong,[∥] Jeong Hee Moon,[⊥] Minwoo Park,[#] Kwangsoo Shin,[†,‡] Sue In Chae,[†,‡] Jisoo Lee,[†,‡] Taegyu Kang,[†,‡] Back Kyu Choi,[†,‡] Jiwoong Yang,[†,‡] Megalamane S. Bootharaju,[†,‡] Hyoin Song,[†,▽], Seong Hee An,[▽] Kyung Man Park,[▽] Joo Yeon Oh,[♦] Hoonkyung Lee,[#] Myung Soo Kim,*[,†,▽] Jungwon Park,*[,†,‡] and Taeghwan Hyeon*[,†,‡]

[†] Center for Nanoparticle Research, Institute for Basic Science (IBS), Seoul 08826, Republic of Korea.

[‡] School of Chemical and Biological Engineering, and Institute of Chemical Process, Seoul National University, Seoul 08826, Republic of Korea.

[∥] UNIST Central Research Facilities (UCRF), Ulsan National Institute of Science and Technology (UNIST), Ulsan 44919, Republic of Korea.

[⊥] Disease Target Structure Research Center, Korea Research Institute of Bioscience and Biotechnology (KRIBB), Daejeon 34141, Republic of Korea.

[#] Department of Physics, Konkuk University, Seoul 05029, Republic of Korea.

[▽] Department of Chemistry, Seoul National University, Seoul 08826, Republic of Korea.

[♦] ASTA, Suwon 07675, Republic of Korea.

[§] H. Chang and B. H. Kim contributed equally to this work.

*e-mail: thyeon@snu.ac.kr (T.H.); jungwonpark@snu.ac.kr (J.P.); myungsoo@snu.ac.kr (M.S.K.)

Table of Contents

Materials and Methods

Chemicals. Iron chloride hexahydrate (98%), 1-decanol, 3-aminoquinone, insulin, and cytochrome C were purchased from Sigma-Aldrich. Sodium oleate (95%) was purchased from TCI. Ethanol, *n*-hexane, chloroform ($CHCl_3$), and *n*-pentane were purchased from Samchum Chem. Peptide Y5R was purchased from Peptron (Daejeon, Korea).

Synthesis of iron-oxo-oleate complex. Iron-oxo-oleate complex was synthesized based on the previously reported method.[S1] Notably, the reaction for the formation of the iron-oxo-oleate complex is not air sensitive (Figure S5). Iron chloride hexahydrate (10.8 g, 40 mmol) and sodium oleate (36.5 g, 120 mmol) were stirred in a mixture of 140 mL hexane, 80 mL ethanol, and 60 mL deionized water for 4 h at 50 °C. The ratio of solvents in a reaction mixture is optimized for clear phase separation.[S2] After the completion of the reaction, the hexane phase was separated using a separation funnel and washed with deionized water three times. Finally, hexane was evaporated under vacuum in overnight.

Synthesis of iron-oxo clusters. Iron-oxo clusters were synthesized by esterification between the iron-oxo-oleate complex and a primary alcohol. First, iron-oxo-oleate complex (1.9 g, 1 mmol) and 1-decanol (10.0 g) were mixed and degassed at room temperature. The mixture was heated to an aging temperature (100 °C to 200 °C) at a heating rate of 3.3 °C/min, and then held at that temperature for 24 h under an inert atmosphere. After the reaction was complete, the solution was rapidly cooled and centrifuged with ethanol to decant unreacted reactants and by-products. The final product was dispersed in non-polar solvents such as hexane or chloroform.

Mass characterization. Mass characterization was performed using a home-built MALDI-TOF instrument. It was calibrated using calibrants, 3-aminoquinone (M_w = 144.17 Da), Y5R peptide (M_w = 990.08 Da), insulin (M_w = 5735.6087 Da), and cytochrome C (M_w = 12361.97 Da), and the matrix 9-nitroanthracene (0.1 M in chloroform). The analyte and matrix were properly mixed in chloroform to obtain optimized mass profiles. The mixture was dried on a sample plate with vacuum evaporation, and the dried samples were desorbed and ionized by a 337-nm nitrogen laser (MNL100, Lasertechnik Berlin, Germany) with an accelerating voltage of 20.0 kV and laser power of 5.0~8.5 μJ. Each spectrum was acquired by focusing 20 laser shots on each spot and 10 different spots were averaged.

Optical characterization. Fourier transform infrared (FT-IR) spectra of the samples were acquired using a Bruker VERTEX 70V spectrometer. The Raman spectra were recorded using a LabRam HV Evolution system equipped with a 514.5-nm Ar-ion laser. The optical absorption spectra were obtained using a CARY 5000E UV-VIS-NIR spectrophotometer.

Solution NMR characterization. Nuclear magnetic resonance (NMR) spectra were recorded on a Bruker Avance III Spectrometer operating at ^{1}H and ^{13}C frequencies of 500.000 MHz and 125.721 MHz. The sample temperature was set as 298.15 K. Fast cooled *ex situ* aliquots were measured without any treatment to avoid losing original information. All samples were dissolved in deuterated chloroform.

TEM characterization. Graphene grown on a Cu foil by CVD (chemical vapour deposition) was placed on a Quanntifoil Au holey carbon grid with a hole size of 1.2 μm. The Cu substrate was etched with 0.1 M aqueous ammonium persulfate solution. The graphene TEM grids were dried at 80 °C overnight and then the cluster solutions were dropped onto the grids. Aberration-corrected transmission electron microscopy (TEM) images were obtained with a TITAN G2 at an acceleration voltage of 80 kV.

***In situ* X-ray scattering measurement & processing.** Synchrotron *in situ* SAXS/WAXS measurements were conducted at the PLS-II 9A U-SAXS beamline of Pohang Accelerator Laboratory (PAL), Korea. The X-rays from the in-vacuum undulator (IVU) were monochromated using Si(111) double crystals and focused at the detector position using K-B-type mirrors (the beam size was 30 μm × 290 μm (V × H)). The scattering patterns were recorded with a 2D CCD detector (Rayonix SX165), and the X-ray irradiation time was 5 s depending on the saturation level of the detector.
For SAXS, the scattering angles were calibrated by a pre-calibrated TiSBA (1st peak at 0.06521 Å^{-1}). The sample-to-detector distance was about 2.0 m. For WAXS, the scattering angles were calibrated by a pre-calibrated sucrose (Monoclinic, P21, a = 10.8631 Å, b = 8.7044 Å, c = 7.7624 Å, β = 102.938°),[S3] and the sample-to-detector distance was about 510 mm.
For the *in situ* experiment, iron-oxo-oleate and primary alcohol were mixed in the same ratio as that in the iron-oxo cluster synthesis and degassed in a vial. The prepared solution was injected into a 1.5-mm quartz capillary tube placed on a heating block. Each experiment was measured at different scattering angles (SAXS or WAXS), aging temperatures, and alcohol chain lengths. The scattering intensities acquired at the SAXS region ($q = 0.015 \sim 0.4$ Å^{-1}) were subtracted by background intensity of excess solvents (1-decanol or diphenyl ether). AUTORG macro was applied to determine the radius of gyration for each subtracted scattering intensity.[S4] The scattering intensity measured within the WAXS region ($q = 2.2 \sim 2.8$ Å^{-1}) can be expressed as the summation of 3rd degree polynomial and the Gaussian distribution.[S5] Here, 3rd degree polynomial refers to the continuously changing background intensity of the solvents and capillary tube. The intensity of the Gaussian distribution originates from the iron oxide nanoparticles.

$$I(q) = aq^3 + bq^2 + cq + d + I_0 \exp(-(q - q_0)^2 / 2\sigma^2)$$

Computational details. The first-principles calculations based on the spin-polarized density functional theory[S6] were performed with the Vienna Ab-initio Simulation Package (VASP) using a projector-augmented-wave (PAW) method.[S7] The exchange correlation energy functional was employed with the generalized gradient approximation (GGA) in the Perdew–Burke–Ernzerhof scheme,[S8] and the kinetic energy cutoff was set as 400 eV. A geometrical optimization of the iron-oxo complexes was carried out until the Hellmann–Feynman force acting on each atom was less than 0.01 eV/Å. To remove spurious interactions between periodic images due to periodic calculations by the long-range Coulomb interaction, a vacuum distance of 15 Å was considered between the molecules.

The formation energy of the iron-oxo complexes was calculated by the following definition: $(E_{\text{Fe-oxo}} - N_{\text{Fe}} \cdot E_{\text{Fe}}^{\text{bulk}} - N_{\text{C}} \cdot E_{\text{C}}^{\text{graphene}} - N_{\text{O}} \cdot E_{\text{O}}^{\text{O}_2} - N_{\text{H}} \cdot E_{\text{H}}^{\text{H}_2})$, where $E_{\text{Fe-oxo}}$, $E_{\text{Fe}}^{\text{bulk}}$, $E_{\text{C}}^{\text{graphene}}$, $E_{\text{O}}^{\text{O}_2}$, and $E_{\text{H}}^{\text{H}_2}$ denote the total energy of the iron-oxo clusters, the total energy per Fe in a bcc Fe, the total energy per C in a graphene, the total energy per O in an O_2 molecule, and the total energy per H in a H_2 molecule, respectively. N_{Fe}, N_{C}, N_{O}, and N_{H} denote the number of iron, carbon, oxygen, and hydrogen atoms for a given cluster, respectively.

Supplementary Figures and Tables

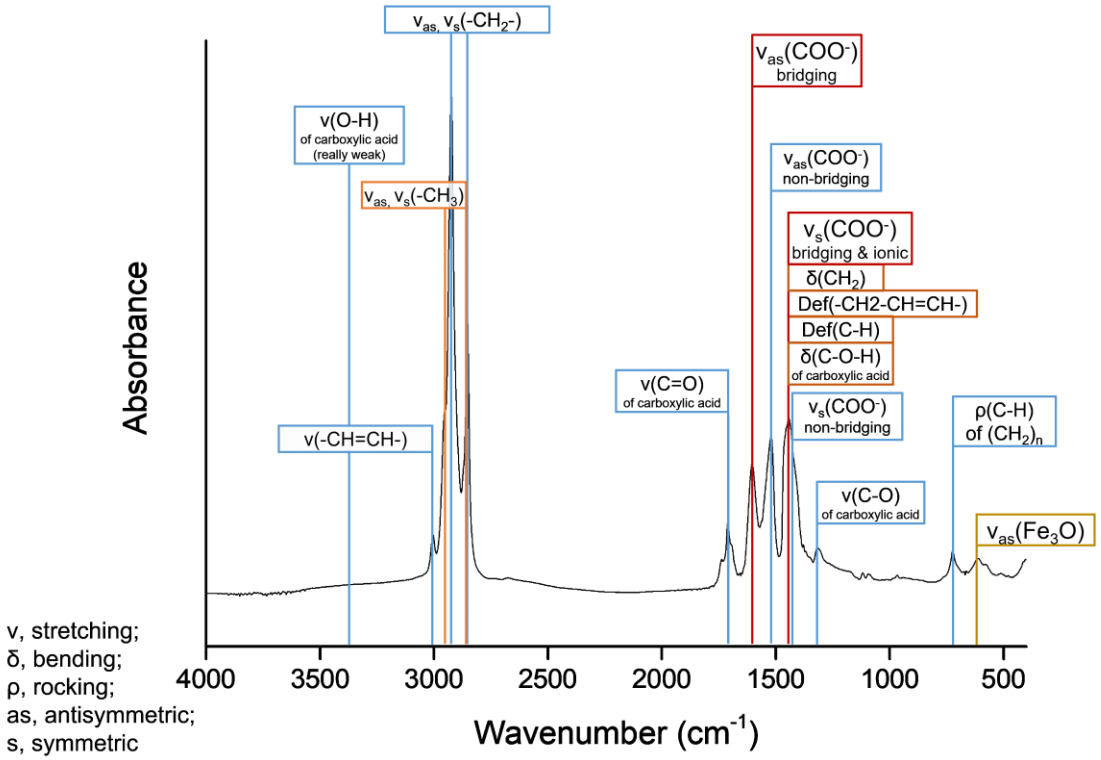

Figure S1. Assignment of peaks in infrared spectrum of iron-oxo-oleate.

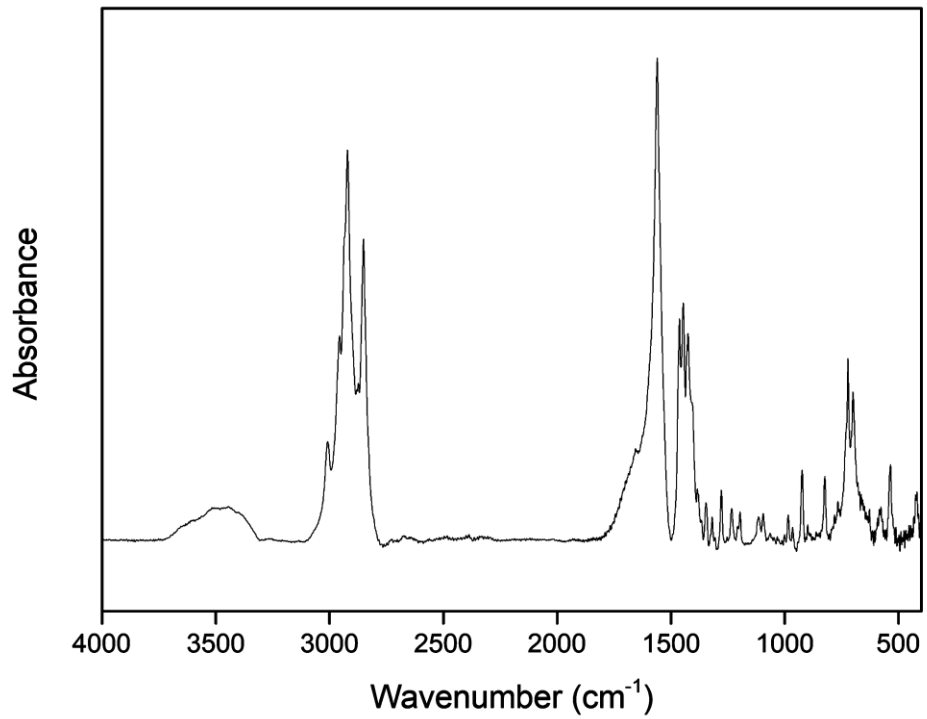

Figure S2. Infrared spectrum of sodium oleate.

As a control experiment, the vibration peaks of sodium oleate are confirmed as 1560 cm^{-1} and 1447 cm^{-1}, which represent the ionic binding mode. The comparison of the FT-IR spectra of iron-oleate complex and sodium oleate reveals that the peaks at 1520 cm^{-1} and 1420 cm^{-1} (shoulder) originate from the asymmetric vibration of non-bridging ionic oleate that binds to the iron-oxo-oleate complex.[S9]

	Iron-oxo-oleate	$[Fe^{III}_3O(acetate)_6]^+ClO_4^-$	$FeCl_3 \cdot 6H_2O$
Absorption wavelength [nm]	935	965	980
Molar absorption coefficient [L mol^{-1} cm^{-1}]	12.8	22.8	0.132

Table S1. Absorption wavelength and molar absorption coefficient of iron complexes.

Elements	Experimental	Calculated
Fe	5.96%	6.04%
C	70.50%	70.18%
H	11.08%	11.09%
O	12.46%	12.69%

Table S2. Elemental composition measured by ICP-MS and elemental analysis. Calculated composition is obtained from the formula $[Fe_3O(C_{18}H_{33}O_2)_6]^+(C_{18}H_{33}O_2)^-(C_{18}H_{33}O_2H)_2(H_2O)_3$.

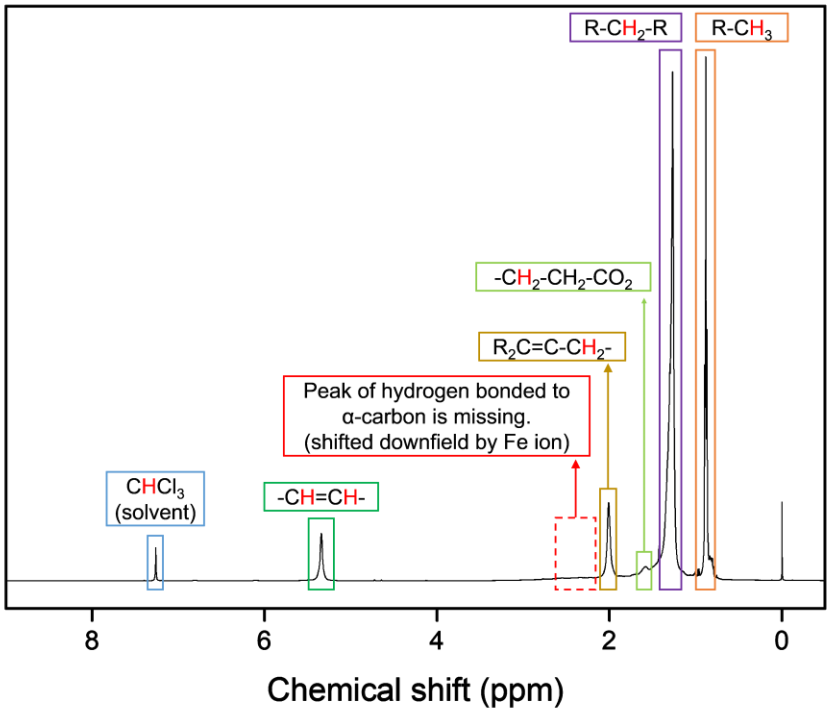

Figure S3. ^{1}H NMR spectrum of iron-oxo-oleate complex.

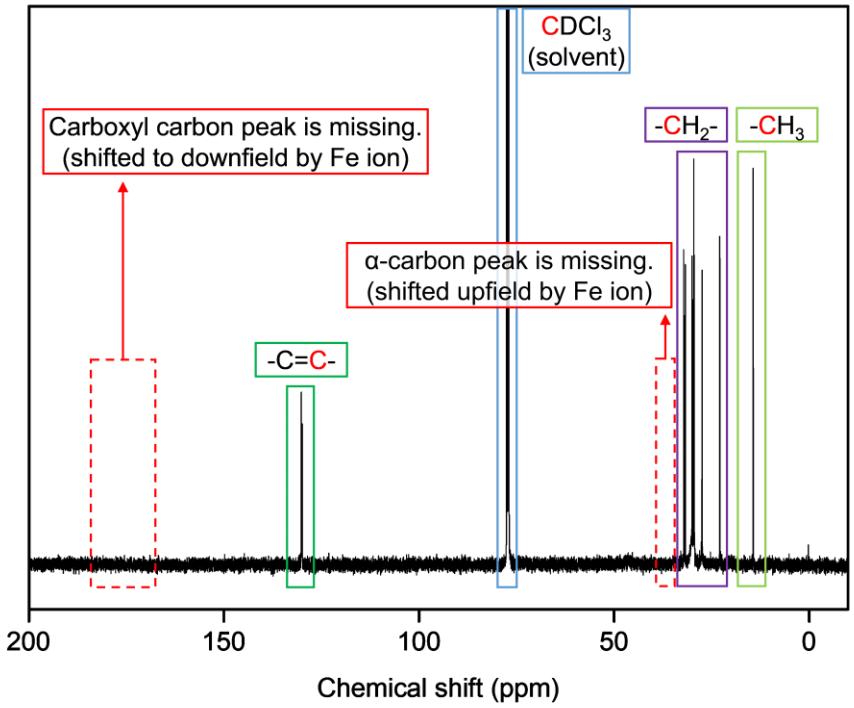

Figure S4. ^{13}C NMR spectrum of iron-oxo-oleate complex.

The direct bonding states of iron ions and oleate ligand induce distinct changes in the NMR spectrum. Carbons and hydrogens, which have 2-bond distance from the iron ions, should not appear in ordinary NMR spectra because paramagnetic iron ions can affect the magnetic resonance of nearby atoms.[S10-11] In the ^{1}H NMR spectrum, hydrogens, which are bonded to the α-carbon of the oleate group, are expected to shift downfield. In the ^{13}C NMR spectrum, the carboxyl carbon is expected to shift downfield, while the α-carbon is shifted upfield.

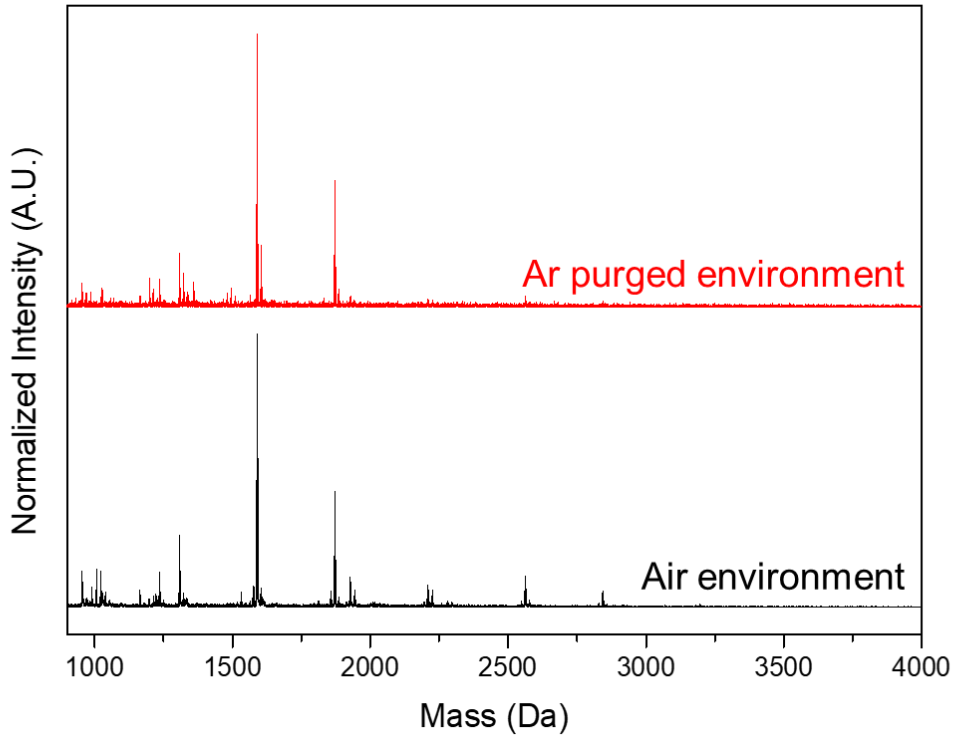

Figure S5. MALDI-TOF MS of iron-oxo-oleate synthesized in air (black) and inert (red) environment.

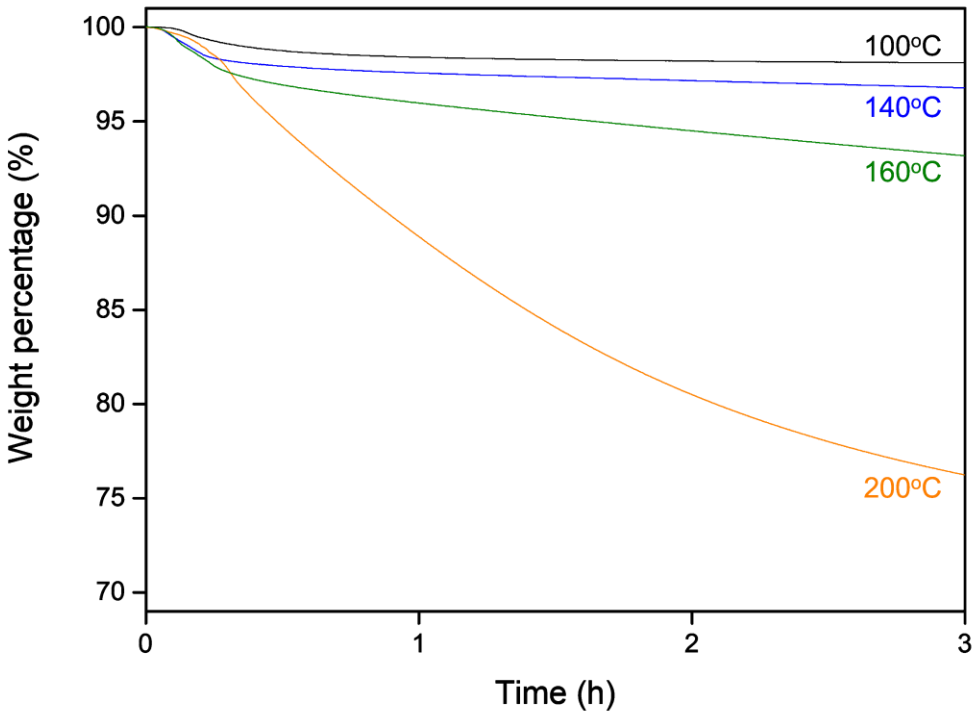

Figure S6. Thermogravimetric analysis (TGA) curve of iron-oxo-oleate measured at different temperatures. TGA confirms that the thermal decomposition of trinuclear-oxo cluster is suppressed below 200 °C.

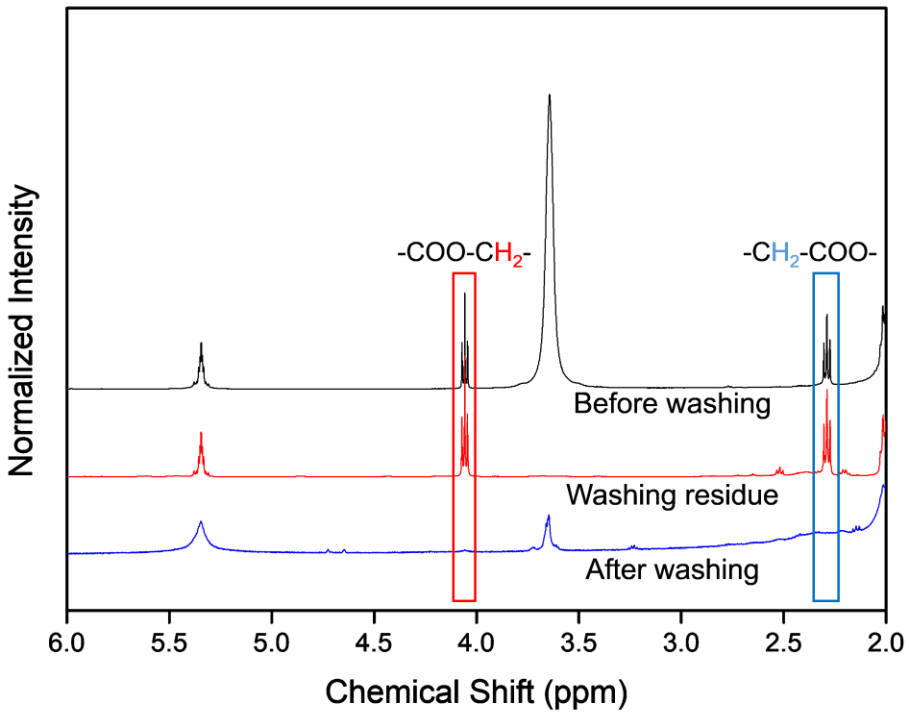

Figure S7. ^{1}H NMR spectra of crude product, washing residue, and final product. Esters are produced after continuous growth and separated after the washing process.

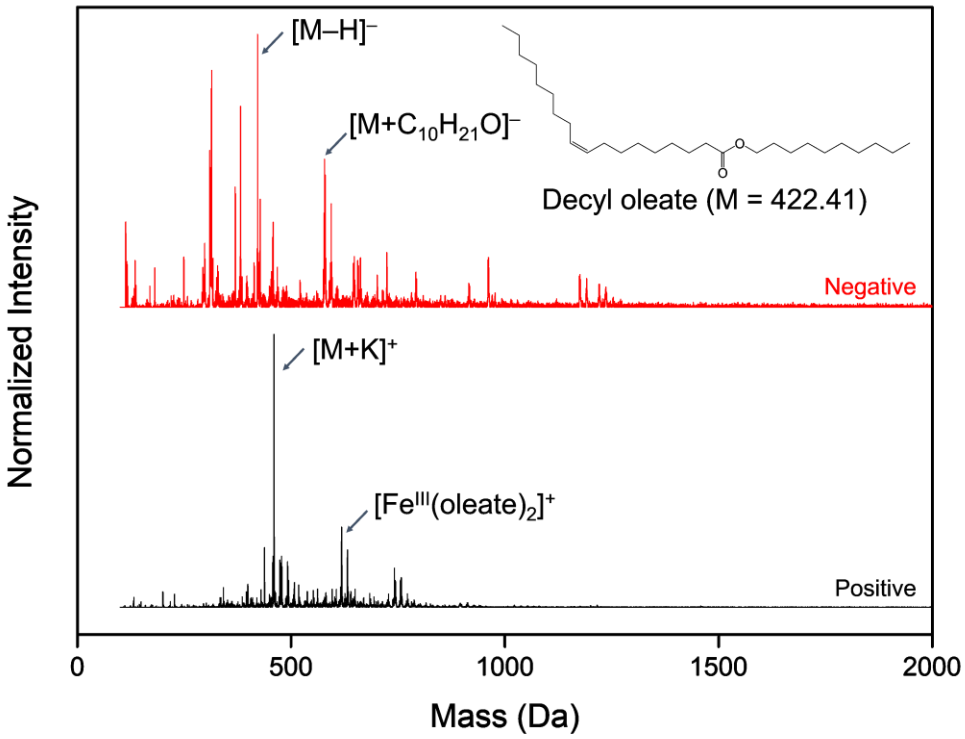

Figure S8. Mass spectrum of decyl oleate in washing solvent analysed by LC-MS.

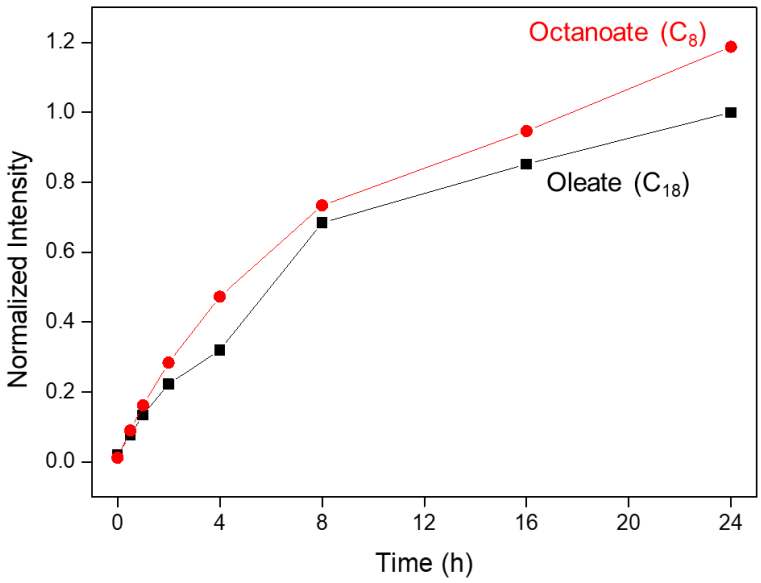

Figure S9. Kinetics of continuous esterification starting from iron-oxo-oleate (black) and iron-oxo-octanoate (red). Absolute quantification of ^{1}H NMR is applied to acquire both plots. At the same temperature, 100 ºC, continuous growth of iron-oxo clusters starting from iron-oxo-octanoate is about 1.15 faster than the case starting from iron-oxo-oleate.

Table S3. Assignment of peaks shown in Supplementary Figure 12. Representative peaks of iron-oxo-oleate are shown in black. Peaks that dramatically emerged after esterification are shown in red. Peaks whose intensities distinctly increased after esterification are shown in green.

	955	1591	1645	1661	1716	1732	1872	1927	1943	2015	2086	2208	2224
Iron	2	3	4	4	5	5	3	4	4	5	6	4	4
Oxygen	0	1	1	2	2	3	1	1	2	3	4	1	2
Oleate	3	5	5	5	5	5	6	6	6	6	6	7	7

	2280	2296	2353	2368	2424	2440	2563	2579	2635	2650	2706	2722	2794
Iron	5	5	6	6	7	7	5	5	6	6	7	7	8
Oxygen	2	3	3	4	4	5	2	3	3	4	4	5	6
Oleate	7	7	7	7	7	7	8	8	8	8	8	8	8

	2844	2860	2916	2932	2988	3004	3194
Iron	5	5	6	6	7	7	6
Oxygen	2	3	3	4	4	5	3
Oleate	9	9	9	9	9	9	10

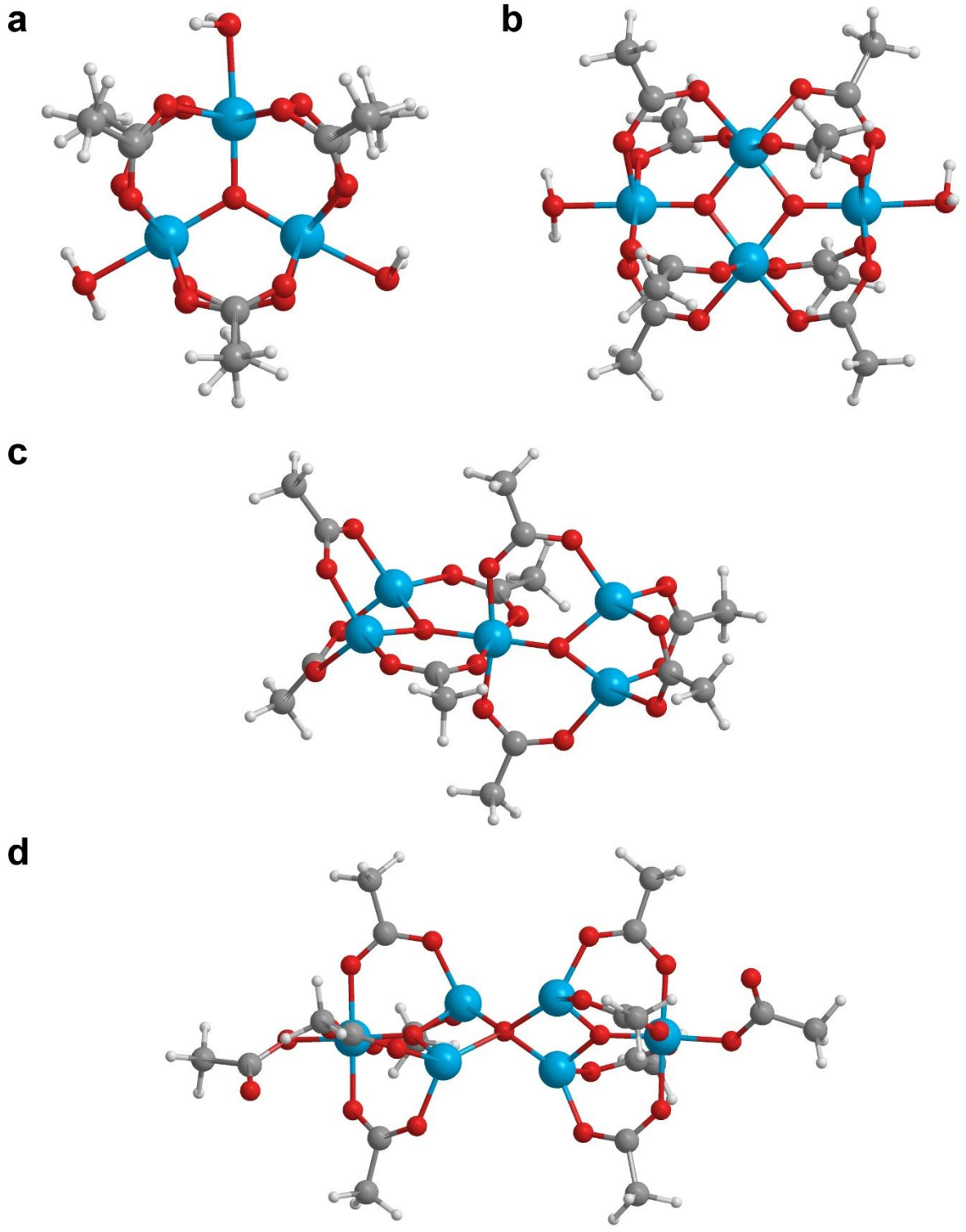

Figure S10. Theoretically derived structures of (a) Fe_3, (b) Fe_4, (c) Fe_5, and (d) Fe_6 clusters calculated by density functional theory.

Number of iron ions	E_{tot}(Iron-oxygen core)	E_{tot}(Iron-oxo clusters)
3	−21.23 eV	−334.80 eV
4	−33.46 eV	−421.15 eV
5	−40.14 eV	−401.14 eV
6	−51.79 eV	−496.02 eV

Table S4. Calculated total energies of iron-oxygen core and iron-oxo clusters.

Number of iron ions	E_f(Iron-oxygen core)	E_f(Iron-oxo clusters)
3	6.44 eV	−49.61 eV
4	6.35 eV	−60.25 eV
5	7.44 eV	−54.74 eV
6	7.91 eV	−62.77 eV

Table S5. Calculated formation energies of iron-oxygen core and iron-oxo clusters.

Number of iron ions	E_b(Iron-oxo clusters)
3	26.80 eV
4	33.76 eV
5	35.51 eV
6	37.35 eV

Table S6. Calculated binding energies of iron-oxo clusters. The total energies of acetate ion and water molecule are −40.687 and −14.217 eV each. Binding energies are calculated by the following formula.

E_b(Iron-oxo clusters) = E_{tot}(Iron-oxygen core) + (# of acetate) × E_{tot}(acetate) + (# of water) × E_{tot}(water) − E_{tot}(Iron-oxo clusters)

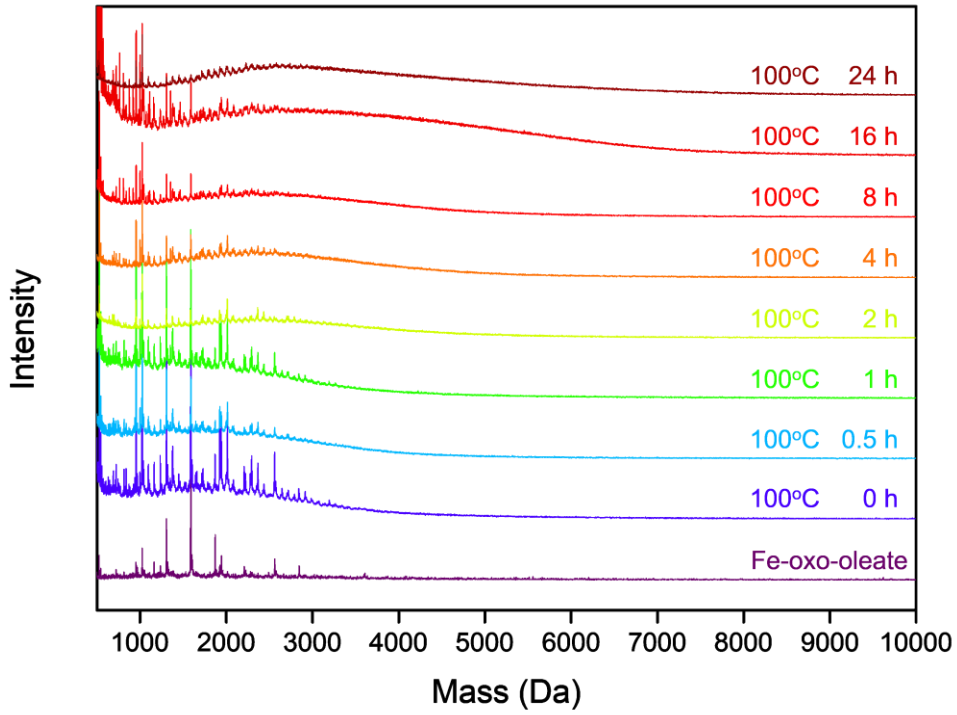

Figure S11. Mass spectra showing continuous growth mechanism at 100 °C.

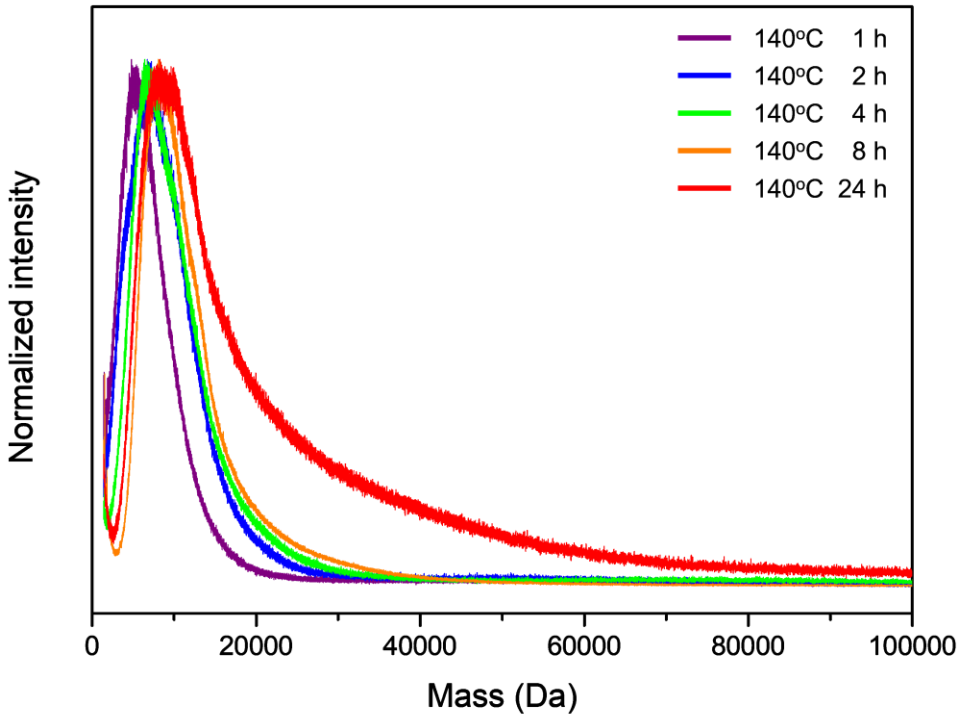

Figure S12. Mass spectra at 140 °C aging condition. After enough aging time, sub-nanometre iron-oxo clusters continuously grow into iron oxide nanoparticles (m/z > 20 kDa).

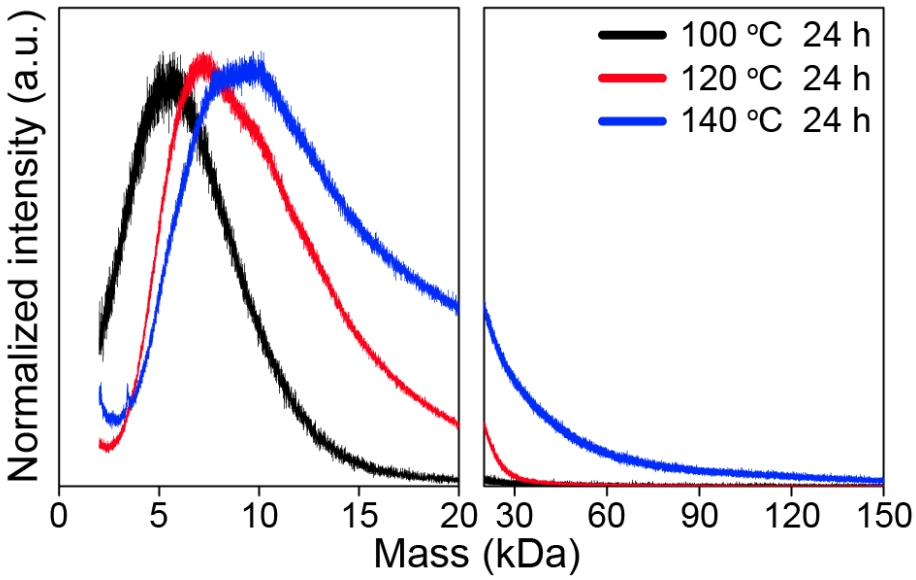

Figure S13. Mass spectra of iron-oxo clusters synthesized for 1 day at different temperatures. Final mass distributions show distinct effect of temperature on the rate of continuous growth.

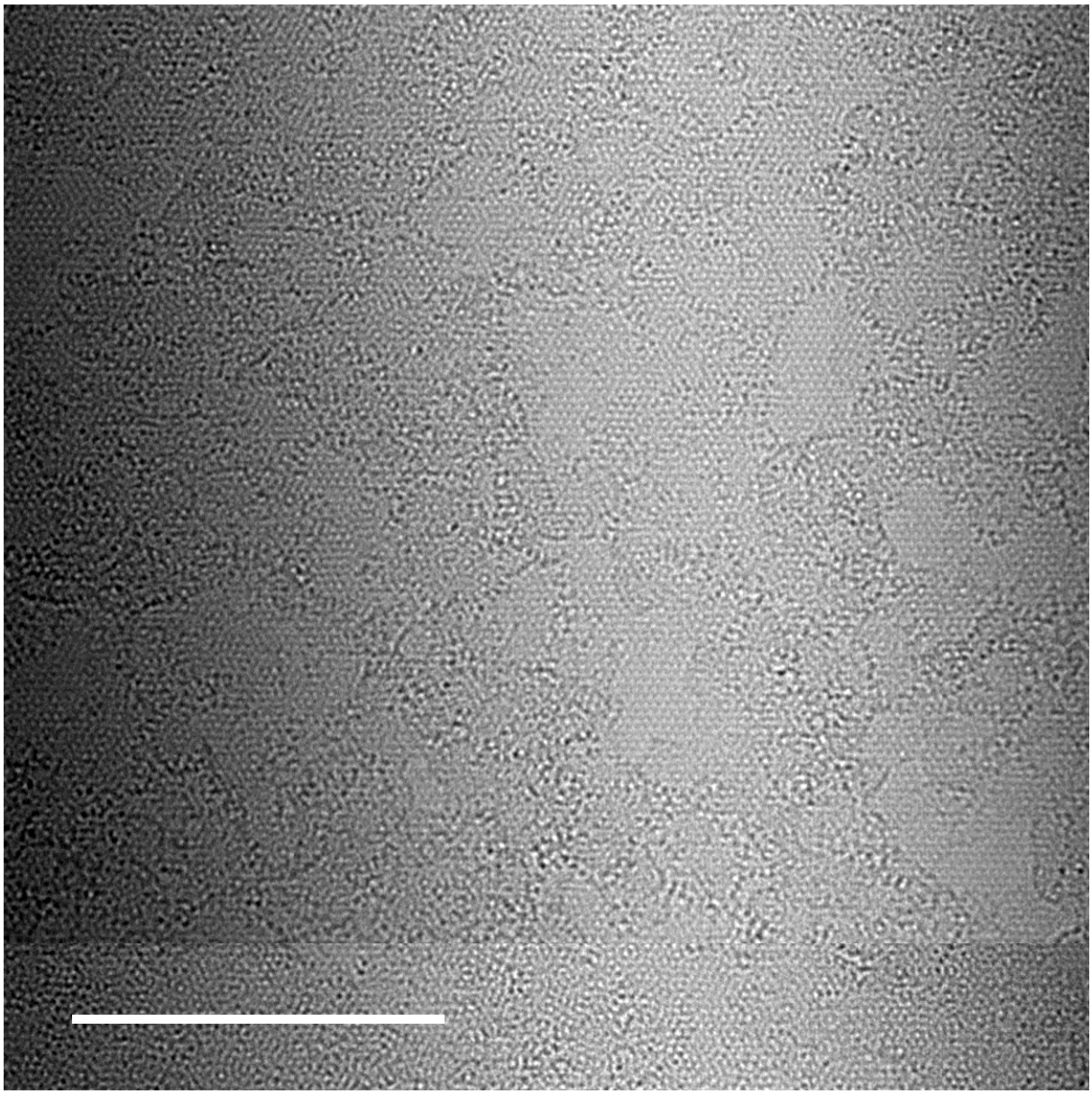

Figure S14. TEM image of iron-oxo clusters acquired from *ex situ* samples at 140 °C 0 h (Figure 5a).

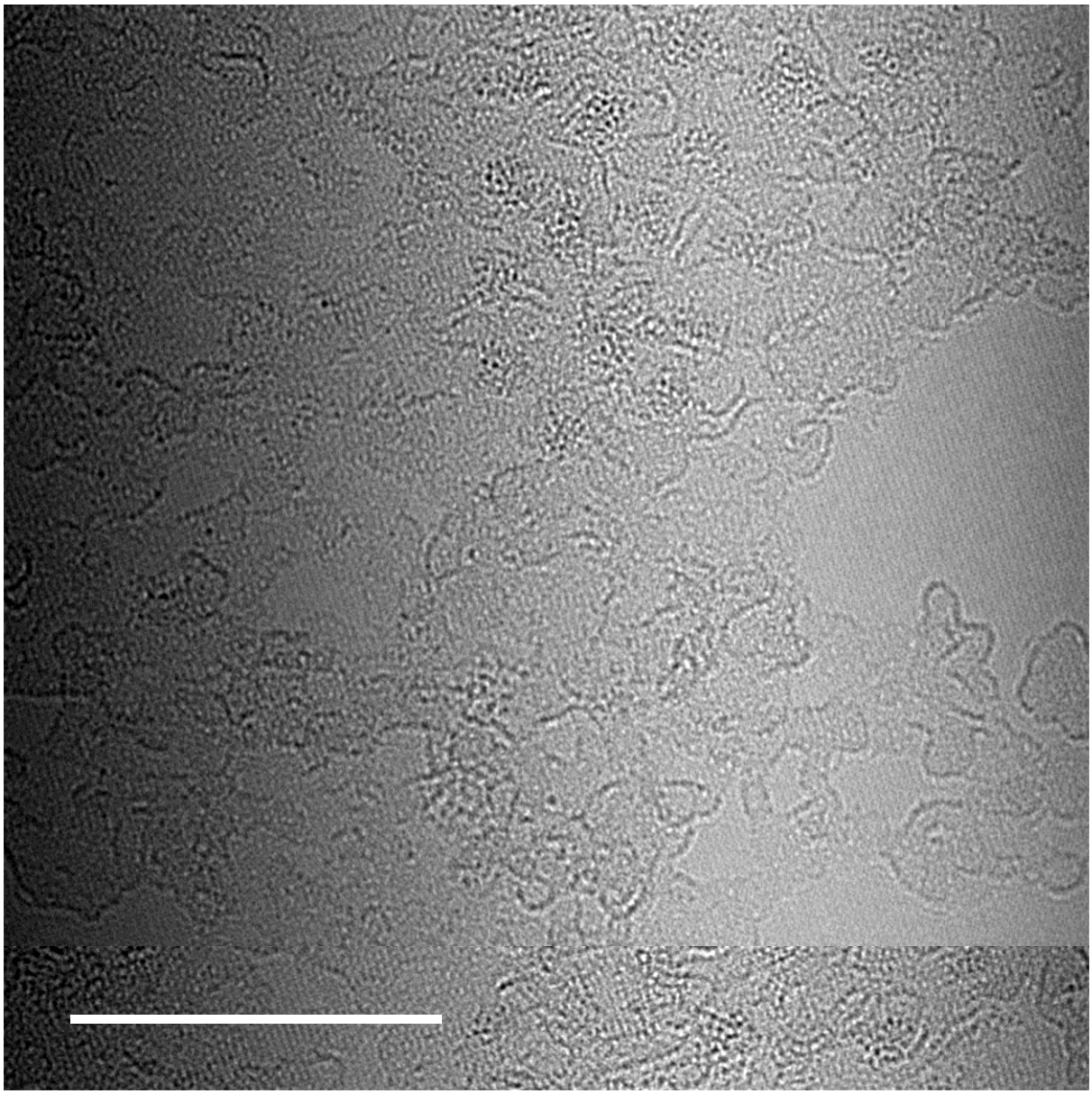

Figure S15. TEM image of iron-oxo clusters acquired from *ex situ* samples at 140 °C 4 h (Figure 5b).

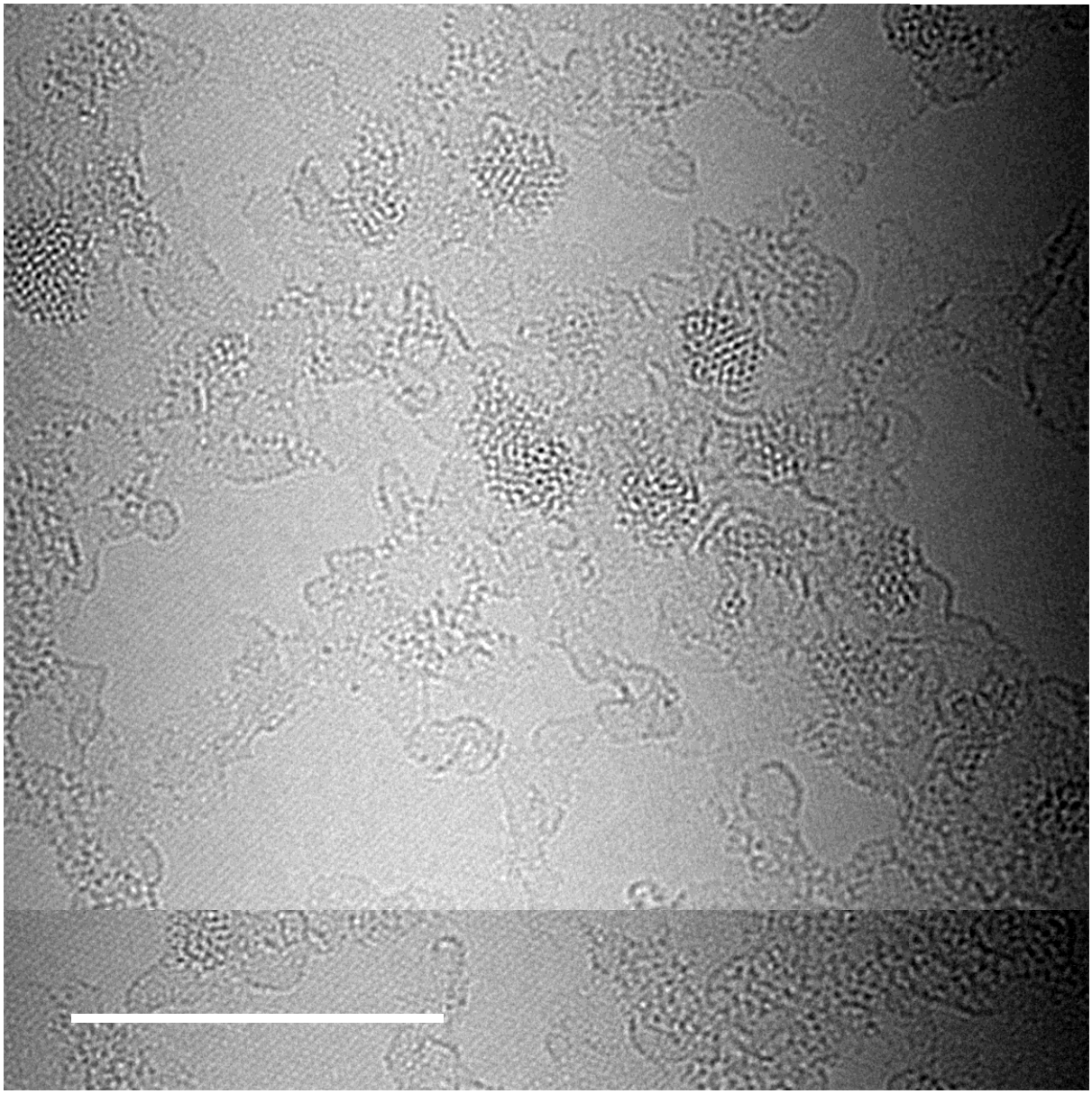

Figure S16. TEM image of iron-oxo clusters acquired from *ex situ* samples at 140 °C 24 h (Figure 5c).

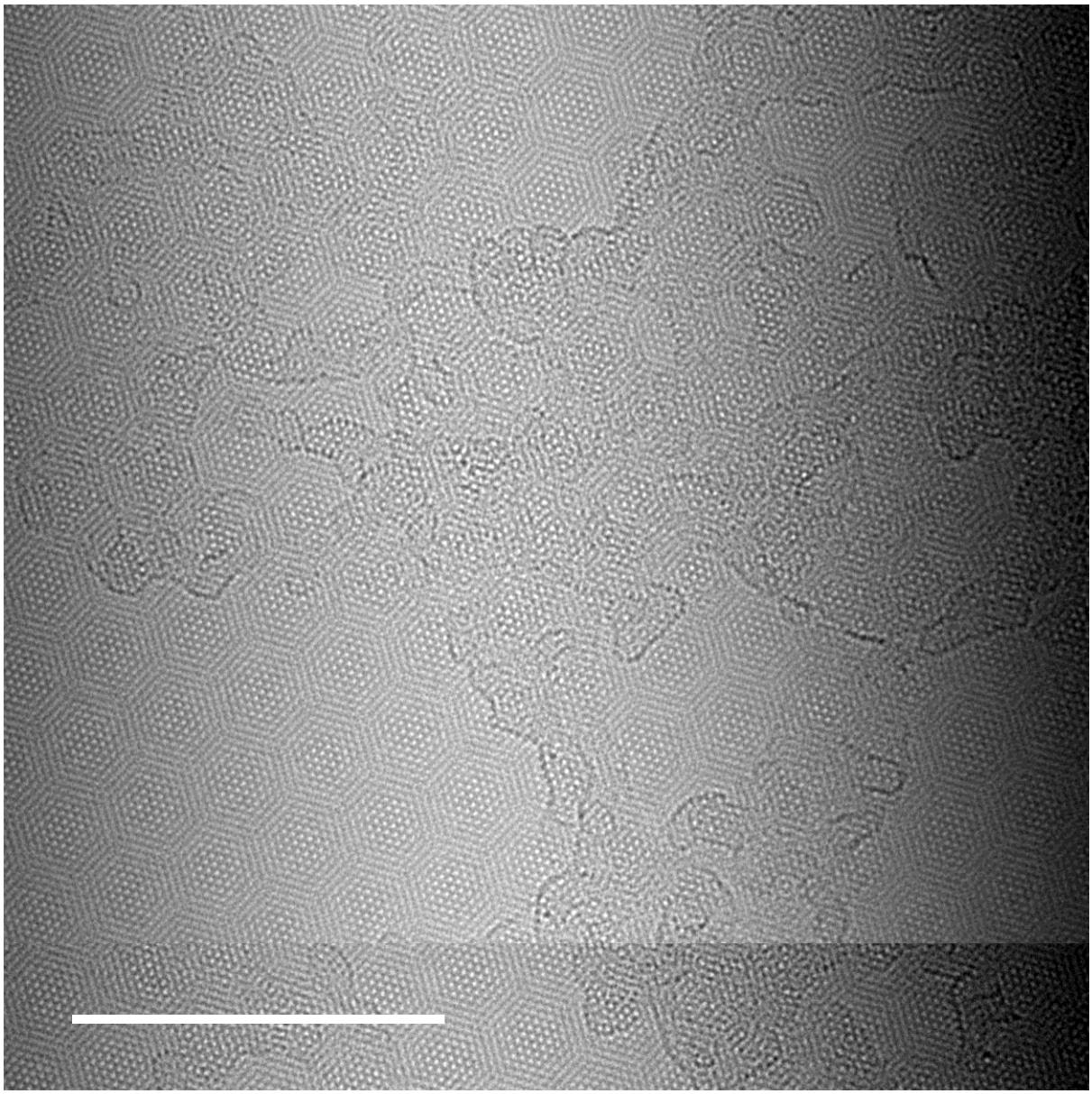

Figure S17. TEM image of graphene substrate loaded without any sample.

Supporting References

(S1) Park, J.; An, K.; Hwang, Y.; Park, J. G.; Noh, H. J.; Kim, J. Y.; Park, J. H.; Hwang, N. M.; Hyeon, T., Ultra-large-scale syntheses of monodispersse nanocrystals. *Nat. Mater.* **2004,** *3*, 891–895.

(S2) Huang, C.; Chung, P.; Tseng, I.-M.; Lee, L., Measurements and Correlations of Liquid-Liquid-Equilibria of the Mixtures Consisting of Ethanol, Water, Pentane, Hexane, and Cyclohexane. *Open Thermodynamics J.* **2010,** *4*, 102–118.

(S3) Hynes, R. C.; Le Page, Y., Sucrose, a convenient test crystal for absolute structures. *J. Appl. Crystallogr.* **1991,** *24*, 352–354.

(S4) Petoukhov, M. V.; Konarev, P. V.; Kikhney, A. G.; Svergun, D. I., ATSAS 2.1 – towards automated and web-supported small-angle scattering data analysis. *J. Appl. Crystallogr.* **2007,** *40*, s223–s228.

(S5) Abecassis, B.; Bouet, C.; Garnero, C.; Constantin, D.; Lequeux, N.; Ithurria, S.; Dubertret, B.; Pauw, B. R.; Pontoni, D., Real-time in situ probing of high-temperature quantum dots solution synthesis. *Nano Lett.* **2015,** *15*, 2620–2626.

(S6) Kohn, W.; Sham, L. J., Self-consistent equations including exchange and correlation effects. *Phys. Rev.* **1965,** *140*, A1133–A1138.

(S7) Kresse, G.; Joubert, D., From ultrasoft pseudopotentials to the projector augmented-wave method. *Phys. Rev. B* **1999,** *59*, 1758–1775.

(S8) Perdew, J. P.; Burke, K.; Ernzerhof, M., Generalized gradient approximation made simple. *Phys. Rev. Lett.* **1996,** *77*, 3865–3868.

(S9) Johnson, M. K.; Powell, D. B.; Cannon, R. D., Vibrational spectra of carboxylato complexes—III. Trinuclear 'basic' acetates and formates of chromium(III), iron(III) and other transition metals. *Spectrochim. Acta A* **1981,** *37*, 995–1006.

(S10) Amani, V.; Safari, N.; Khavasi, H. R., Solution and solid state characterization of oxo-centered trinuclear iron(III) acetate complexes $[Fe_3(\mu_3\text{-}O)(\mu\text{-}OAc)_6(L)_3]^+$. *Spectrochim. Acta A* **2012,** *85*, 17–24.

(S11) Belmore, K.; Madison, X. J.; Harton, A.; Vincent, J. B., Carbon-13 NMR studies of oxo-centered trinuclear chromium(III) complexes of the general formula $[Cr_3O(O_2CR)_6(L)_3]^+$ (R = Me, Ph; L = H_2O, py). *Spectrochim. Acta A* **1994,** *50*, 2365–2370.